Supplementary Figure 1. Fpr1 is expressed in the gastrointestinal tract and influences cAMP. (A) Levels of fMLF levels in the plasma of germfree animals on NCD (n = 3), compared to conventional NCD animals (n = 3). **(B)** Levels of fMLF levels in the colon of germfree animals on NCD (n = 4), compared to conventional NCD animals (n = 8). (**C**) Relative Fpr1 gene expression in various tissues of lean 16-week old WT NCD mice (eWAT = epididymal white adipose tissue; SVF = stromal vascular fraction; BAT = brown adipose tissue). (**D**) Relative Fpr1 gene expression in the small intestinal lamina propria, colon, and pancreatic islets isolated from WT animals fed either NCD or HFD (n = 3). (**E**) Chemotaxis of thioglycolate-elicited intraperitoneal macrophages (IP-Macs) in response to fMLF (250 nM) is suppressed by co-incubation with Pertussis Toxin (PT), an inhibitor of Gi-coupled signaling. (**F**) Relative cAMP levels in forskolin-stimulated IP-Macs are reduced by treatment with fMLF. (**G**) Relative transcript levels of four related Fpr genes in the colon of WT and Fpr1-KO mice on NCD and HFD (n = 6 mice per group). (**H**) Relative transcript levels of related Fpr genes in the ileum of WT and Fpr1-KO mice on NCD and HFD. Data = mean ± SEM. ns = not significant. # = below detection limit. *P<0.05, **P<0.001, ***P<0.0001 by two-tailed t test (**D**) or One-way ANOVA and Bonferroni's post-test (**E-H**), comparing the indicated groups.

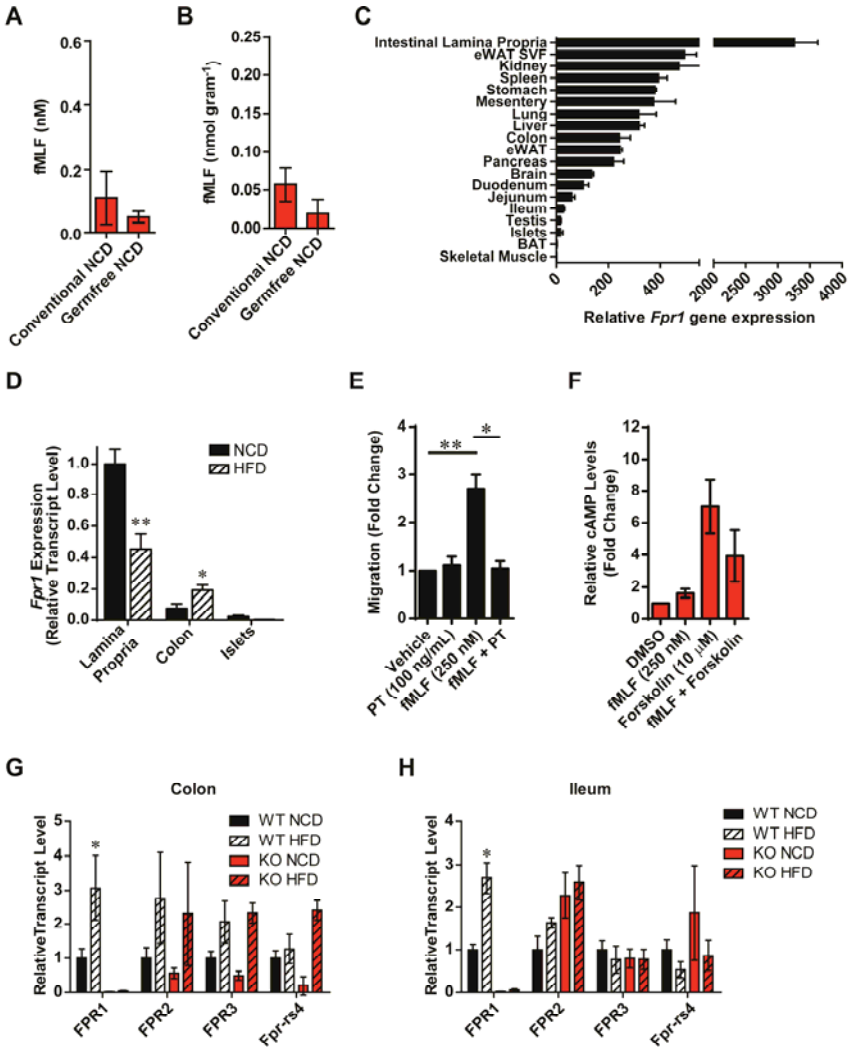

Supplementary Figure 2. Obese/HFD Fpr1-KO mice do not display significant differences in weight gain or organ weight (**A**) Body weight gain of WT and Fpr1-KO littermates on 60% HFD (*n* = 7-10 mice per group). (**B**) Food intake. (**C-F**) Weight of epididymal white adipose tissue, liver, pancreas, and spleen of mice after 13 weeks on HFD. (**G**) Intestine length (**H-I**) weight of the colon and cecum after contents were removed. (**J**) Area of insulin-positive islets as a percentage of the pancreas, an estimation of beta cell mass, in HFD WT and Fpr1-KO littermates (*n* = 6-7 mice per group). (**K**) Average islet size (*n* = 6-7 mice per group). Data = mean ± SEM.

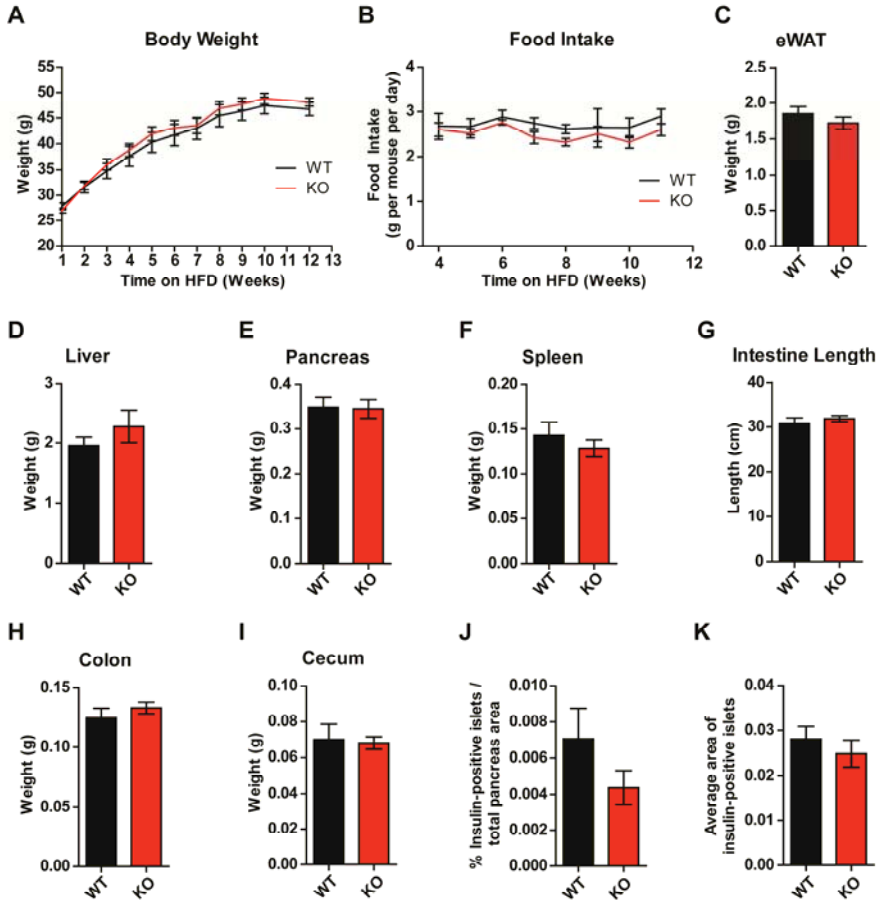

Supplementary Figure 3. Loss of Fpr1 does not significantly improve glucose tolerance in lean/NCD animals. (**A-B**) OG-GTT of WT and Fpr1-KO littermates at 16 weeks of age, and corresponding AUC (*n* = 6-10 mice per group). (**C**) Body weight of the mice at the time of the OG-GTT. (**D-E**) Insulin levels and basal GLP-1 levels measured during the OG-GTT. (**F**) IP-ITT at 17 weeks of age. Data = mean ± SEM.

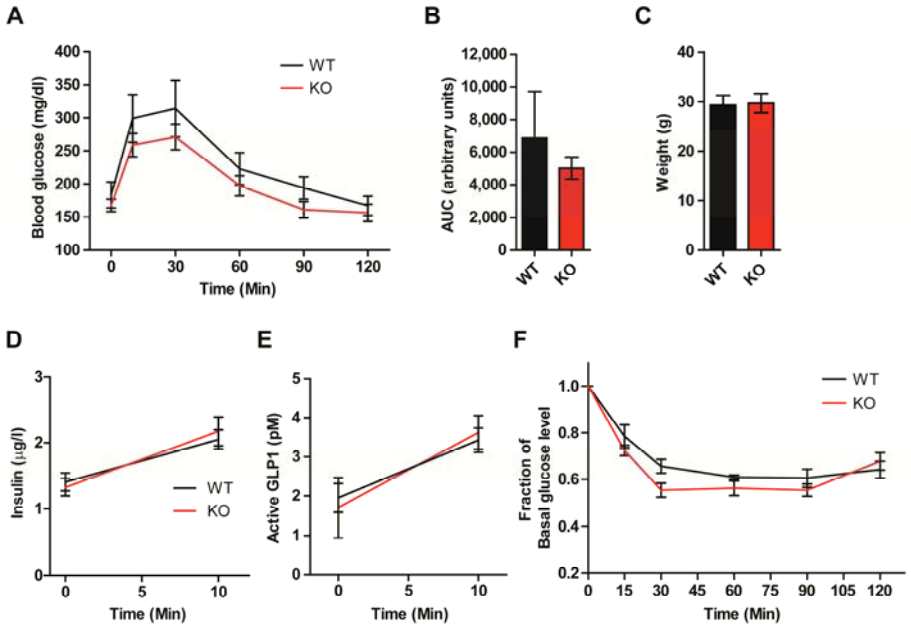

Supplementary Figure 4. Analysis of basal glucagon and gastric hormone levels in obese/HFD animals. (**A**) Basal fasted blood plasma glucagon levels measured immediately prior to OG-GTT in HFD WT and Fpr1-KO littermates (n = 9 mice per group). (**B-H**) Active GLP-1, Total GLP-1, Peptide YY (PYY), Gastric Inhibitory Polypeptide (GIP), Leptin, Ghrelin, and Resistin levels in the basal fasted state measured immediately prior to OG-GTT (n = 7-10 mice per group). Data = mean ± SEM. ns = not significant. *P<0.05, by two-tailed t test.

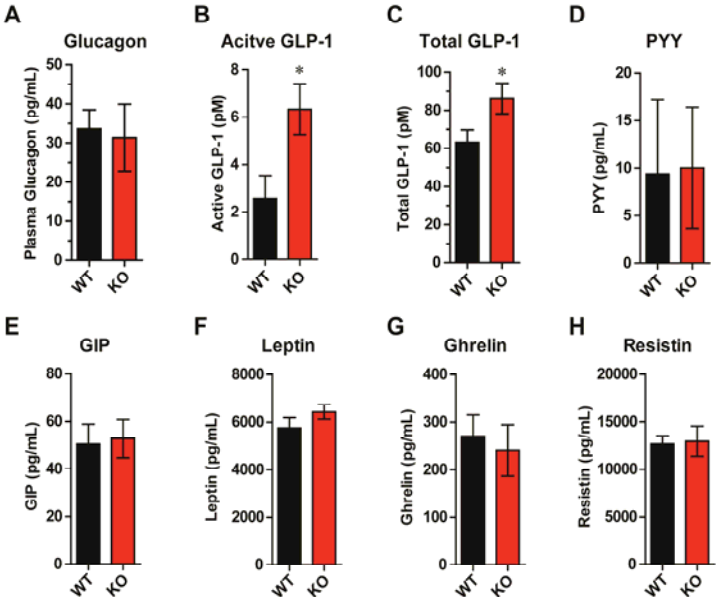

Supplementary Figure 5. Oral treatment with broad-spectrum antibiotics improves glucose tolerance and increases GLP-1 levels. (**A**) OG-GTT of WT HFD animals after daily oral gavage of broad-spectrum antibiotics for two weeks (n = 8 mice per group). (**B**) Basal active GLP-1 levels measured immediately prior to OG-GTT. (**C**) Basal insulin levels prior to OG-GTT. Error bars = s.e.m. n.d. = not detectable. *P<0.05 by One-way ANOVA with Bonferroni's post-test.

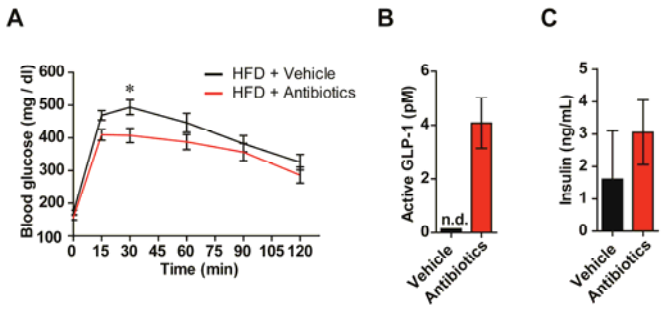

Supplementary Figure 6. fMLF Acts upon Fpr1 on L-cells to modulate GLP-1 secretion in obese/HFD animals. (**A**) Quantification of GLP-1 immunofluorescence labeling in the ileum of WT and Fpr1-KO animals on NCD and HFD (n = 8). (**B**) Ileum *proglucagon* transcript levels in Fpr1-KO HFD animals relative to WT HFD (n = 8). (**C**) Relative mRNA levels of *proglucagon* in the colon of WT and Fpr1-KO HFD mice. (**D**) Relative *Fpr1* mRNA expression in *Proglucagon*-positive L-cells as detected by RNA-fluorescence *in situ* hybridization in colon sections from NCD and HFD animals (n = 4). (**E**) Immunofluorescence staining of GLP-1 and FPR in L-cells of WT HFD colon sections (representative images, scale bars = 10 μm). (**F**) Western immunoblot of FPR and HSP90 in colon tissue lysates of WT NCD versus HFD animals, normalized densitometry quantification shown in (**G**) (n = 3 per group). (**H**) siRNA knockdown of *fpr1* transcript levels in mGLUTag cells (n = 5). (**I**) mRNA transcript levels of *fpr1, il-1β* and *proglucagon* in mGLUTag cells treated with or without 400 μM palmitate for 24 hours (n = 3). Data = mean ± SEM., ns = not significant. **P*<0.05, ***P*<0.001, ****P*<0.0001 by One-way ANOVA with Bonferroni's post-test (**A and D**) or two-tailed *t* test.

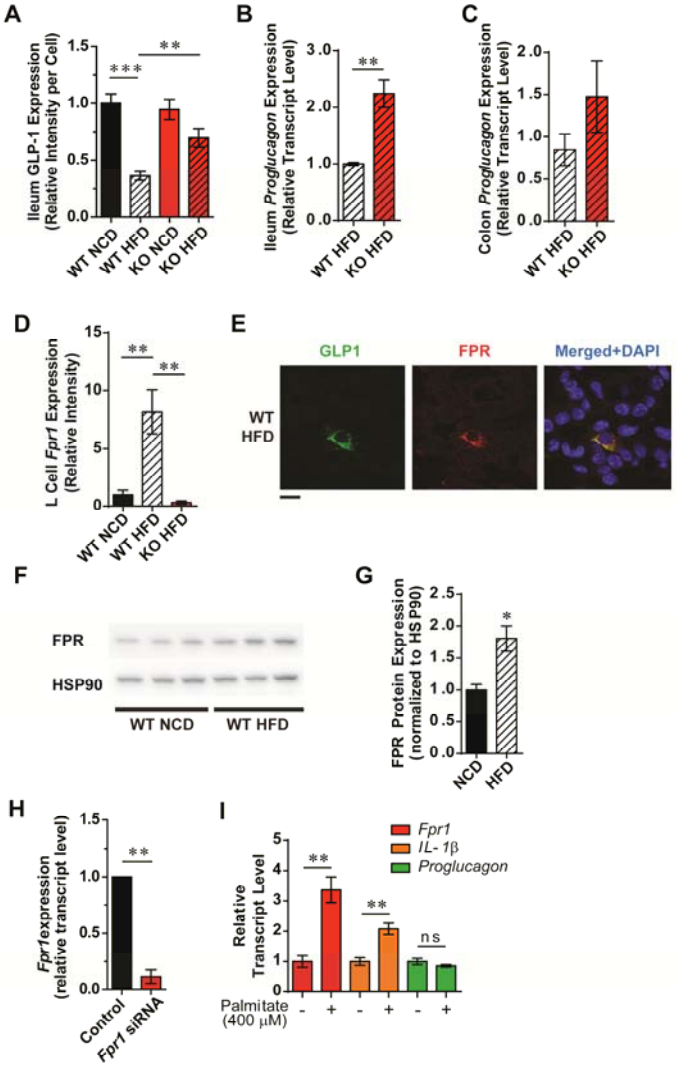

Supplementary Figure 7. Intestinal leukocyte composition and inflammatory gene expression in WT and Fpr1-KO mice. (**A**) Total CD11b+ leukocytes in the small intestinal lamina propria isolated from WT and Fpr1-KO littermates on NCD and HFD (percentage of CD45+ cells) (n = 6 mice per group). (**B**) MHCII- SigletF+ eosinophils (**C**) MHCII+ SigletF- macrophages (**D**) CD11b- CD11c+ dendritic cells (**E**) CD45+ CD3+ T cells (**F**) CD8+ T cells (**G**) CD4+ T cells (**H**) CD4+ Foxp3+ Treg cells. (**I**) mRNA transcript levels of pro-inflammatory *TNF*□, *ALOX5*, and *IL1β* in immune cells of the small intestinal lamina propria from WT and Fpr1-KO littermates (n = 4-6 mice per group). (**J**) mRNA transcript levels of IL-10 (n = 4-6 mice per group). (**K**) Levels of circulating chemokines and cytokines in the blood plasma of WT and Fpr1-KO mice (n = 8-9 mice per group). Data = mean ± SEM. ns = not significant. *P<0.05, **P<0.001, ***P<0.0001 by One-way ANOVA and Bonferroni's post-test.

SUPPLEMENTARY DATA

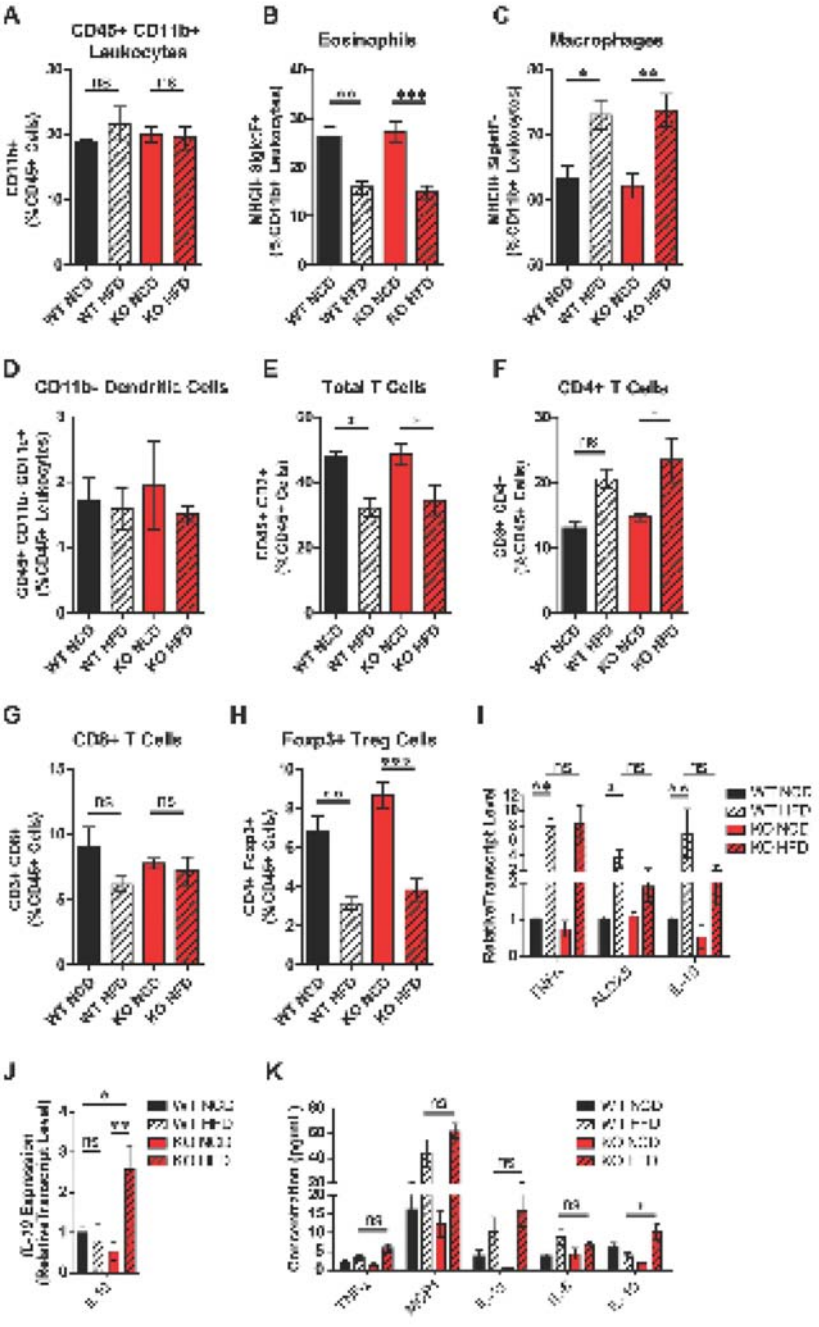

Supplementary Figure 8. Analysis of inflammation in epididymal white adipose tissue of WT and Fpr1-KO mice on HFD. (A) Mac-2 staining of eWAT sections (representative images, n = 8 mice per group, scale bar = 250 μm). (**B**) FACS analysis of F4/80+ macrophages isolated from eWAT tissue. (**C**) mRNA transcript levels of pro-inflammatory "M1-type" genes in eWAT. (**D**) mRNA transcript levels of IL-10. Data = mean ± SEM. *P<0.05, **P<0.001, ***P<0.0001 by two-tailed t test.

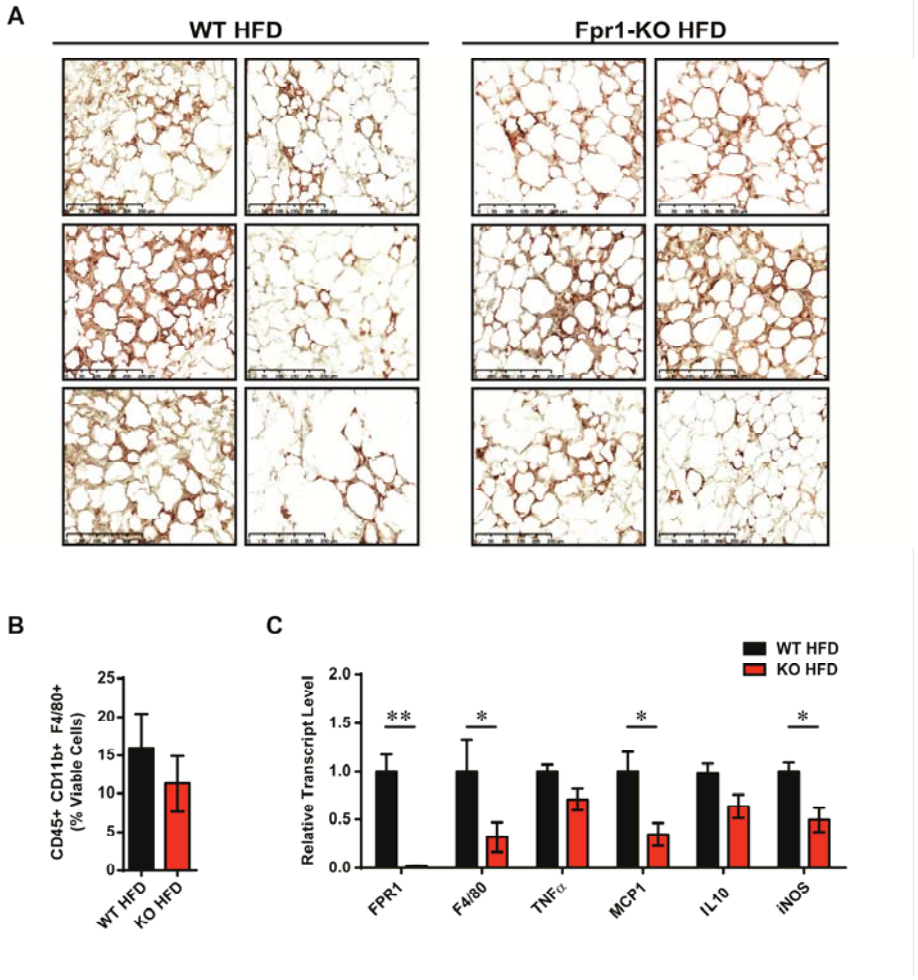

Supplementary Figure 9. (**A**) OG-GTT of WT NCD animals after daily oral gavage with the Fpr1 agonist fMLF for 2 weeks (1 mg/kg) (n = 8 mice per group). (**B**) Matrix-assisted laser desorption-time of flight (MALDI-TOF) mass spectra of synthesized Fpr1 antagonist cFLFLF, positive ion mode. (**C**) Body weight of WT HFD mice during daily oral gavage treatment with the Fpr1 antagonist cFLFLF (0.5 mg/kg) or vehicle for three weeks (n = 8 mice per group). (**D**) Food intake during antagonist treatment. (**E-H**) Weight of epididymal white adipose tissue, liver, pancreas, and spleen upon sacrifice. Data = mean ± SEM. ns = not significant. *P<0.05, **P<0.001 by two-tailed t test.

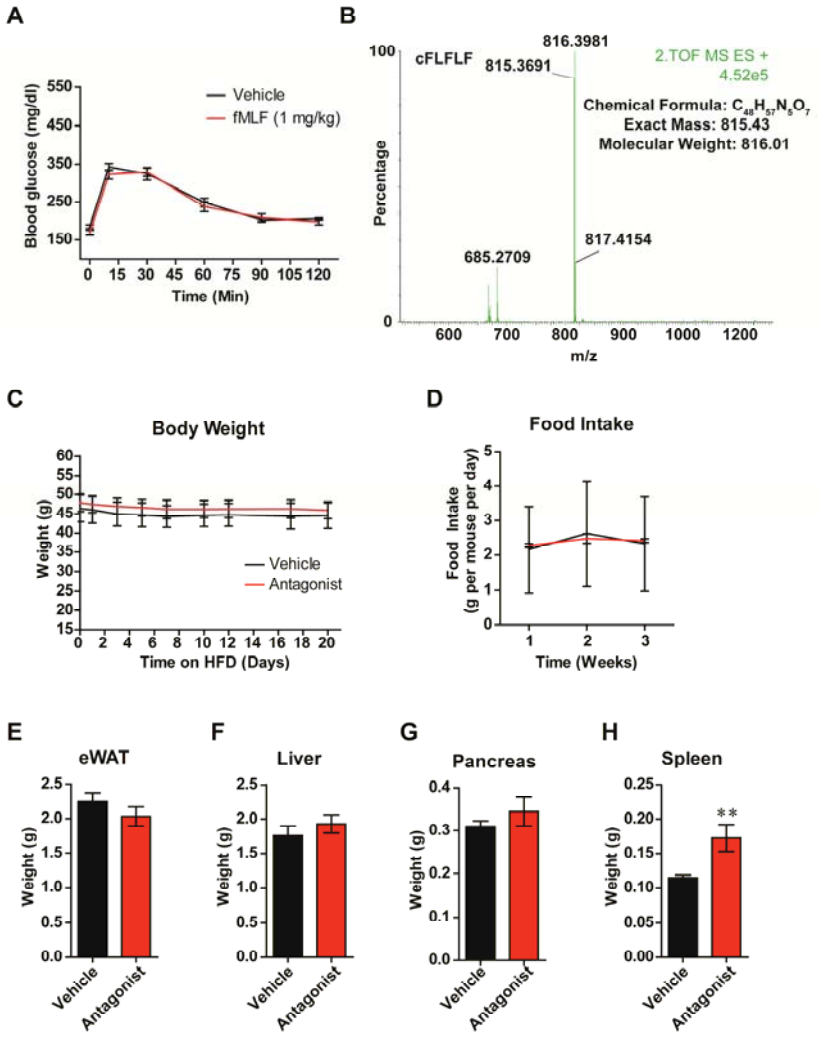

Supplementary Figure 10. Analysis of intestinal permeability and microbiome composition in WT and Fpr1-KO littermates. (**A)** Analysis of fecal albumin levels in WT and Fpr1-KO littermates (*n* = 12-18 mice per group). (**B**) Blood plasma FITC-Dextran levels in lean/NCD and obese/HFD mice (*n* = 4-6 mice per group). (**C**) A second measure of alpha diversity, OTU richness, confirms that Fpr1-KO mice on HFD have significantly increased microbiome diversity within each sample compared to WT animals on HFD. Legend also applies to (**D-H**). (*n* = 6-10 mice per group). (**D**) Mean relative abundance of members of the Phylum Bacteroidetes within each sample. (**E**) Mean relative abundance of members of the Phylum Firmicutes within each sample. (**F**) Mean relative abundance of members of the Family Lactobacillaceae within each sample. (**G**) Mean relative abundance of members of the Family Lachnospiraceae within each sample. WT animals on HFD display increased abundance of this Family compared to NCD, whereas Fpr1-KO animals on HFD have significantly lower levels, resembling NCD. (**H**) Mean relative abundance of members of the Family Rikenellaceae within each sample. WT animals on HFD have reduced abundances compared to NCD, whereas Fpr1-KO animals on HFD have significantly elevated levels compared to WT **(***n* = 6-10 mice per group). (**I**) Log 2-fold change of bacterial pathways predicted altered by inferred metagenomics content analysis, according to Kyoto Encyclopedia of Genes and Genomes (KEGG) orthology (*n* = 6-10 mice per group). (**J**) Analysis of Bray-Curtis dissimilarity distances between Fpr1-KO and WT HFD microbiome samples, from 3 cohorts of HFD microbiome samples, comparing mice housed separately or co-housed. Data = mean ± SEM. ns = not significant. **P*<0.05, ***P*<0.001, ****P*<0.0001 by One-way ANOVA and Bonferroni's post-test (A-B) or PERMANOVA and DESeq 2 (D-H, J).

SUPPLEMENTARY DATA

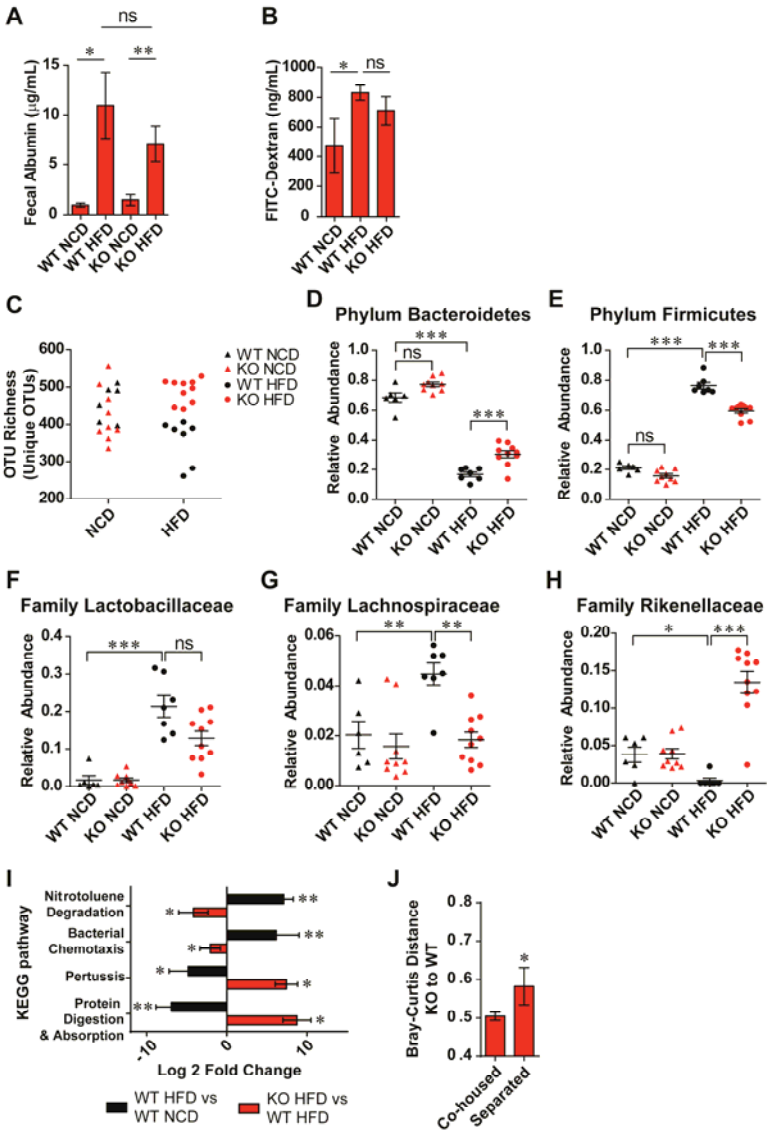

Supplementary Figure 11. Model of microbiota-produced fMLF action upon GLP-1 secretion and glucose tolerance in diet-induced obesity. (**A**) In lean NCD conditions, a healthy intestinal microbiota produces low levels of *N*-formyl peptides including fMLF. After a meal, glucose in the intestine is taken up by L-cells in the intestinal epithelium, stimulating production and secretion of extra-pancreatic GLP-1 by these cells into systemic circulation, which promotes glucose tolerance through both insulin-dependent and independent mechanisms, including suppression of gastric emptying, reduced glucagon production, CNS effects and neuronal signaling from the gut to the brain. In this paradigm, the effects of GLP-1 from either α-cells or L-cells to stimulate insulin secretion would represent only one arm of GLP-1 regulation of glucose homeostasis. (**B**) In obese HFD conditions, intestinal dysbiosis leads to increased *N*-formyl peptide levels, and L-cells express higher levels of FPR1. Increased intestinal permeability in HFD animals also leads to elevated levels of *N*-formyl peptides entering circulation. In the gut, *N*-formyl peptides activate FPR1 on L-cells to suppress GLP-1 secretion, leading to reduced glucose tolerance.